

Coronary Inflammation by Computed Tomography Pericoronary Fat Attenuation in MINOCA and Tako-Tsubo Syndrome

Nicola Gaibazzi, MD, PhD; Chiara Martini, RT; Andrea Botti, MD; Antonio Pinazzi, MD; Barbara Bottazzi, RT; Anselmo A. Palumbo, MD

Background—The pericoronary fat attenuation index (pFAI) has emerged as a marker of coronary inflammation, which is measurable from standard coronary computed tomography angiography (CCTA). It compares well with gold-standard methods for the assessment of coronary inflammation and can predict future cardiovascular events. pFAI could prove invaluable to differentiate an inflammatory from a noninflammatory coronary artery status, helping unravel the mechanisms subtending an event classified as myocardial infarction with nonobstructive coronary arteries (MINOCA) or Tako-Tsubo syndrome (TTS).

Methods and Results—Patients admitted with MINOCA and TTS between 2011 and 2018, who had both CCTA and cardiac magnetic resonance during or shortly after the acute phase, were selected and pFAI measured in their CCTA; pFAI was also measured in control subjects who had CCTA for atypical chest pain workup, no obstructive coronary artery disease found in their CCTA, and no cardiac events at 2-year follow-up. In the $n=106$ MINOCA/TTS patients, mean pFAI was -68.37 ± 8.29 versus -78.03 ± 6.20 in the $n=106$ controls ($P<0.0001$), and the difference was confirmed also when comparing mean pFAI in each coronary artery between MINOCA/TTS and controls ($P<0.0001$). Nonobstructive coronary plaques at CCTA, high-risk plaques in particular, were more frequently found ($P<0.01$) in the MINOCA/TTS group compared with controls.

Conclusions—In MINOCA and TTS patients, CCTA is not only able to detect angiographically invisible atherosclerotic plaques, but its diagnostic yield can be expanded using the simple measurement of pFAI to characterize pericoronary fat tissue; in MINOCA/TTS mean pFAI demonstrates higher values compared with controls, a finding that has been associated with coronary artery inflammation. (*J Am Heart Assoc.* 2019;8:e013235. DOI: 10.1161/JAHA.119.013235.)

Key Words: computed tomography • coronary artery disease • coronary inflammation • MINOCA • pericoronary fat attenuation • Tako-Tsubo syndrome

An imaging biomarker that could noninvasively assess coronary artery inflammation would be invaluable for research and clinical use.¹ The detection of coronary artery inflammation would allow personalized risk assessment in patients with suspected coronary artery disease (CAD), beyond clinical data, coronary stenosis severity or presence of high-risk plaques, allowing the initiation of maximized risk reduction strategies in truly high-risk patients.² The pericoronary fat attenuation index (pFAI) has recently emerged as a clinical marker of coronary inflammation that is easy to

measure from standard coronary computed tomography angiograms (CCTAs).³ It compares well with gold-standard techniques for the assessment of plaque inflammation,⁴ and it is able to predict future cardiovascular events, at least in patients with suspected stable CAD.⁵

Myocardial infarction with nonobstructive coronary arteries (MINOCA) is a working diagnosis, recognizing several possible mechanisms. The definition of MINOCA of the European Society of Cardiology working group is based on the absence of overt clinical causes for an acute myocardial infarction (MI) in which coronary angiography demonstrates no or $<50\%$ coronary artery stenosis.⁶ In a percentage of MINOCA, a cause can be finally identified, although it may become apparent only after thorough multimodality diagnostic workup.

pFAI could prove useful to differentiate an inflammatory from a noninflammatory coronary artery status, helping unravel the mechanism subtending a MINOCA event. Coronary artery vasospasm, for example, has been clearly associated with coronary inflammation.⁷

In the current study, we retrospectively selected patients with MINOCA and Tako-Tsubo syndrome (TTS) (the recent American Heart Association scientific statement considers

From the Cardiology and Radiology Departments, Parma University Hospital, Parma, Italy.

An accompanying Data S1 is available at <https://www.ahajournals.org/doi/suppl/10.1161/JAHA.119.013235>

Correspondence to: Nicola Gaibazzi, MD, PhD, Parma University Hospital, Via Gramsci, 14, 43124 Parma, Italy. E-mail ngaibazzi@gmail.com

Received May 10, 2019; accepted August 7, 2019.

© 2019 The Authors. Published on behalf of the American Heart Association, Inc., by Wiley. This is an open access article under the terms of the Creative Commons Attribution-NonCommercial-NoDerivs License, which permits use and distribution in any medium, provided the original work is properly cited, the use is non-commercial and no modifications or adaptations are made.

Clinical Perspective

What Is New?

- In the current single-center study we compared for the first time peri-coronary fat attenuation index using computed tomography angiography, which is an index associated with vascular inflammation, between a group of patients with myocardial infarction with nonobstructive coronary arteries or Tako-Tsubo and controls.
- Patients with MINOCA and Tako-Tsubo demonstrated significantly higher values of pericoronary fat attenuation index compared with controls, indicating that inflammation is associated with such diseases, although typical obstructive atherosclerotic coronary artery disease is absent or trivial in these subjects.

What Are the Clinical Implications?

- Computed tomography angiography could be used from a diagnostic standpoint not only to assess coronary artery plaques, but, in the absence of obstructive disease or significant high-risk plaques, it could also confirm the clinical suspicion of an atypical coronary artery disease syndrome through the finding of inflamed coronary arteries.
- We speculate that this newly available diagnostic tool in the future may help select patients for new therapies, for example, therapies targeting coronary inflammation, and have a measurable feedback regarding their efficacy.

TTS as a separate entity)⁸ who were clinically investigated with both CCTA and cardiac magnetic resonance (CMR) at the time of or shortly after their event.

We measured pFAI in all patients with MINOCA and TTS and compared it with healthy controls, who had a CCTA for atypical chest pain workup (with no obstructive CAD or cardiac events during their follow-up), to assess the relative contribution of inflammation in MINOCA and TTS.

Methods

The data that support the findings of this study are available from the corresponding author upon reasonable request.

Patients

The study was approved by the Institutional Review Board and Research Ethics Committee, and all subjects gave written informed consent. We screened patients who were admitted to our institution from January 2011 to January 2018, had invasive coronary angiography, and were finally discharged (or eventually died) with a diagnosis of MI. The definition of MI was as follows: (1) typical chest pain lasting >20 minutes; (2) persistent electrocardiographic changes; and (3) at least one

troponin I value above the 99th percentile upper reference limit with a rise and/or fall in serial measurements.

MINOCA cases

Patient inclusion required (1) a confirmed diagnosis of MI; (2) an available invasive coronary angiogram in the acute phase showing no or <50% coronary artery stenosis; (3) no identifiable clinically overt cause for the acute MI event; (4) CCTA performed within 7 days after the MI event; and (5) CMR performed within 2 weeks, which excluded findings compatible with myocarditis.

Exclusion criteria for MINOCA cases were (1) a history of previous MI or coronary revascularization or cardiac surgery or cardiomyopathy or severe valvular disease; (2) noncardiac disease potentially linked to troponin I elevations (pulmonary embolism, end-stage renal disease, severe anemia); or (3) low technical quality CCTA and/or CMR, as visually assessed by 2 experienced operators.

TTS cases

Patient inclusion criteria were the same used for MINOCA cases, but additionally they had to fulfill the European Society of Cardiology–Heart Failure Association diagnostic criteria for TTS.⁹ They were required to show left ventricular ballooning (either apical, midcavity, or basal) and modest cardiac biomarker release; the partial or complete recovery of left ventricular ejection fraction to normal values at 6-month follow-up echocardiography was required to confirm the TTS diagnosis. Exclusion criteria were CMR showing findings compatible with myocarditis, the presence of acute or chronic infectious diseases or other inflammatory conditions such as flulike illness, any pyrexial illness or septic presentation, asthma, eczema, allergy, rheumatoid arthritis, systemic lupus erythematosus, Crohn disease, ulcerative colitis, or any concurrent physical illness that in the judgment of investigators was a potential confounder to the hypothesis (eg, concurrent hypertrophic or noncompaction cardiomyopathy, moderate to severe left ventricular hypertrophy of any cause).

Controls

A control group, comprising consecutive subjects presenting to CCTA for workup of atypical acute chest pain, after being evaluated in our the chest pain unit, since January 2011, and showing no or <50% coronary artery stenosis at CCTA was selected using the same exclusion criteria applied to MINOCA/TTS cases; additionally, subjects who had any cardiovascular event (ischemic or arrhythmias) at a minimum follow-up of 2 years after their index CCTA were also excluded.

Coronary Angiography

Selective conventional coronary angiography was performed in all cases (MINOCA/TTS) using standard techniques (Innova

2000 GE; General Electric, Milwaukee, WI). Standard multiple projections were recorded for the left and right coronary arteries. Left ventriculography was performed in the right oblique projection. All of the coronary angiograms were evaluated by an experienced angiographer. The severity of coronary stenosis was visually estimated, as was the presence of calcifications and subtle changes in lumen contour.

Coronary Computed Tomography

CCTA examinations were performed using a Dual Source computed tomography (CT) system (Somatom Definition FLASH; Siemens Healthcare, Forchheim, Germany). See Data S1 for detailed CCTA image acquisition parameters. To achieve optimal image quality and reduce the radiography dose, all patients with a heart rate >65 bpm received intravenous atenolol 5 to 10 mg 5 minutes before the CT scan to reduce motion artifacts. Low and regular heart rates allowed to scan patients using the prospective ECG scan technique or high-pitch FLASH CT protocol. All patients received sublingual nitrates (isosorbide dinitrate 0.5 mg/tablets administered 1–3 minutes before the investigation) to improve visualization of the coronary arteries by dilation.

CCTA analysis—coronary artery anatomy and plaque analysis

The data set was analyzed by 2 experienced readers using an offline workstation software package (Leonardo; Siemens Medical Solutions, Forchheim, Germany).

Angiographic CT data sets of the reconstructed coronary vessels were created in the best phase of the cardiac cycle depending on the heart rate of the patient (end-diastolic cardiac phase usually set at 60% of the R-R interval or end-systolic phase set at 30% of the R-R interval). The presence of plaques was assessed using original axial images, multiplanar reconstruction, and cross-sectional reconstruction. All of the coronary segments were analyzed in accordance with the American Heart Association classification,¹⁰ and each segment was delimited by identifiable side branches. We defined high-risk plaque features (positive remodeling, spotty calcification, napkin-ring sign, low-attenuation plaque) as previously described.¹¹

Pericoronary Fat Attenuation Index

To measure the perivascular pFAI, we used a software package (Aquarius Workstation version 4.4.13; TeraRecon Inc., Foster City, CA), and we traced proximal 40-mm segments of the 3 major epicardial coronary vessels (for right coronary artery starting 10 mm distal to the ostium, while for left anterior descending artery and circumflex artery starting normally at the ostium)⁵ and defined perivascular fat

as the adipose tissue within a radial distance from the outer vessel wall equal to the diameter of the vessel. We ascertained the perivascular fat attenuation index by quantifying the weighted perivascular fat attenuation after adjustment for technical parameters (if 100-kV voltage was used instead of 120-kV voltage, the mean Hounsfield unit [HU] value was corrected dividing by 1.11485) on the basis of the attenuation histogram of perivascular fat within the range –190 to –30 HU, as described previously⁵ (see Data S1 for details on pFAI measurement).

Cardiac Magnetic Resonance

All of the CMR studies were acquired using a 1.5 T magnetic resonance imaging system (Philips Achieva; Philips Medical System, Best, The Netherlands), commercially available cardiac CMR software, vector electrocardiographic triggering, and a dedicated 5-channel phase-array surface coil. The image parameters in detail can be found in Data S1. All CMR studies were analyzed using an offline workstation (ViewForum, Philips Medical Systems). The late gadolinium enhancement (LGE) images were analyzed by 2 experienced readers for the presence and localization of MI, which was defined as a hyperintense area whose signal intensity was >5 SDs greater than that of the remote myocardium¹² and whose subendocardial or transmural distribution was compatible with coronary distribution. Lake Louise criteria were used to exclude myocarditis.¹³

Definition of Infarct-Related Artery

For each MINOCA patient, excluding TTS, the infarct-related culprit artery (IRA) was assigned on the basis of the LGE location shown by the CMR images or, if LGE was not present, using acute wall motion abnormalities at CMR or echocardiography; the association between coronary artery distribution and myocardial segments was made on the basis of the American Heart Association recommendations.¹⁰ IRA was not even assigned in TTS patients because of wall motion abnormalities typically crossing the boundaries of coronary artery territories in this syndrome.

Transthoracic Echocardiography

Echocardiography was performed in MINOCA/TTS during hospital stay, with commercially available ultrasound scanners (iE33; Philips Medical Systems, Andover, MA) and analyzed by an experienced cardiologist. Three cardiac cycles in each of the standard parasternal long-axis; short-axis; and apical 4-, 3-, and 2-chamber views were obtained at a frame rate of at least 40 Hz and offline analysis performed for left ventricular ejection fraction and wall motion abnormalities. In suspected

TTS cases, echocardiograms performed at 5 to 7 months after the event were additionally reviewed to confirm the temporary nature of the acute wall motion abnormalities.

Statistical Analysis

The normally distributed continuous variables were expressed as mean values and SD, and compared using the *t*-test for independent samples; the continuous variables that were not normally distributed were expressed as median values and interquartile range and compared with the Mann–Whitney *U* test. The categorical values were expressed as numbers and percentages and compared using the chi-square test. The association between nonnormally distributed continuous variables was assessed with linear regression. Logistic regression was used to test the association between dichotomous variables and pFAI ≥ -70.1 HU, which is the previously published cutoff for coronary inflammation in subjects with suspected CAD.⁵ We will also derive the best pFAI cutoff to identify MINOCA/TTS versus controls from our data set, by identifying the value that maximized Youden's *J* statistic (sum of sensitivity and specificity) on receiver operating characteristic curve analysis. The intraclass coefficient was used to assess intra- and interobserver reliability/agreement of pFAI measurement. A $P < 0.05$ was considered significant. The statistical analyses were made using Statsdirect software, version 3.0 (<http://www.statsdirect.com>. England: StatsDirect Ltd.; 2013.).

Results

Population

Of 3482 patients admitted to our tertiary center with MI diagnosis between January 2011 and January 2018, $n=177$ patients with confirmed MI did not show any coronary artery disease or $<50\%$ diameter stenosis at invasive coronary angiography; among them, $n=118$ (66%) had both CCTA and CMR available, but according to selection criteria for MINOCA/TTS cases, $n=3$ were excluded because of a history of prior MI, $n=6$ were excluded because reclassified by CMR data to a final diagnosis of myocarditis and $n=3$ were excluded for low-quality CCTA (motion artifacts). The final MINOCA/TTS group was composed of $n=106$ subjects.

The MINOCA/TTS group could be further divided into 3 subgroups based on (1) absence of an identifiable or suspected mechanism for the specific MINOCA event ($n=63$), (2) MINOCA with suspected coronary artery dissection (SCAD) at invasive coronary angiography ($n=17$), or (3) TTS ($n=26$). The same overall number of controls ($n=106$) were selected from our CCTA database and their exams assessed with the same methods used for MINOCA/TTS.

Table 1 reports and compares demographics, risk factors, ECG, peak troponin I, left ventricular wall motion data,

CMR-LGE, and CCTA data in MINOCA/TTS and controls. Hypertension was more frequent in the MINOCA/TTS group, while cigarette smoking was more frequent in controls; the demographic variables and the rest of clinical variables were not significantly different between the 2 groups. The number of patients with at least 1 coronary plaque defined as high risk (according to predefined CCTA criteria) was significantly higher in MINOCA/TTS cases ($n=55$, 52%) compared with controls ($n=33$, 31%) ($P=0.003$).

Pericoronary Fat Attenuation Index

Mean pFAI, averaged for the 3 coronary arteries in the MINOCA/TTS group ($n=106$) was -68.37 ± 8.29 HU, while in the control group it was -78.03 ± 6.20 HU, showing a statistically significant difference ($P < 0.0001$). Figure 1 graphically shows mean pFAI averaged over the 3 coronary arteries in MINOCA/TTS and the difference versus pFAI controls ($P < 0.0001$), and also shows the mean pFAI values in each of the 3 coronary arteries in the MINOCA/TTS group ($P=ns$). Figure 2 graphically shows the paired comparison of mean pFAI for each single coronary artery between MINOCA/TTS and controls, demonstrating a significant difference with higher pFAI in MINOCA/TTS versus controls in each coronary artery ($P < 0.0001$). Dichotomized pFAI ($<$ or ≥ -70.1 HU, according to the previously reported best cutoff for coronary inflammation)⁵ was not associated with any demographic or clinical variable, presenting symptom, presenting ECG (ST-segment–elevation MI versus non–ST-segment–elevation MI) or the presence of an identifiable IRA, wall motion abnormalities, left ventricular ejection fraction, CMR-LGE, or the finding of at least 1 high-risk coronary plaque (Logit $P=ns$ for all). There was no significant association between pFAI and Agatston calcium score ($r=0.065$, $P=0.508$) and also between pFAI and peak troponin I ($r=0.146$, $P=0.134$).

Table 2 reports CCTA data on coronary artery plaques and pFAI and fat volume in detail, measured in each coronary artery, both in the MINOCA/TTS and control study groups. Patients with at least 1 coronary plaque were $n=64$ (60%) in the MINOCA/TTS group and $n=42$ (40%) ($P=0.004$). Plaque characteristics used to define high-risk plaques are here also reported separately, demonstrating that low-attenuation plaques in particular were almost 6 times more frequent in the MINOCA/TTS group compared with controls ($P < 0.0001$).

Mean pFAI in the control group was significantly higher in the left circumflex coronary artery, compared either with the right coronary artery ($P=0.024$) or left anterior descending artery ($P=0.001$), but in the MINOCA/TTS there was no significant difference ($P=ns$) among the mean pFAI of the 3 coronary arteries. In the MINOCA/TTS group, the mean pFAI of each coronary artery versus the other were significantly associated ($r=0.531$, $r=0.602$, $r=0.701$, all with $P < 0.0001$);

Table 1. Demographics, Clinical Characteristics, Medications, Cardiac Imaging, and CCTA Data in Patients With MINOCA and Healthy Controls

Demographics	MINOCA/TTS (n=106)	Controls (n=106)	P Value
Age, median (lower-upper quartile), y	65 (51–73)	63 (48–68)	ns
Female sex, n (%)	62 (42)	52 (49)	ns
BMI, kg/m ²	26.24 (4.6)	27.13 (4.5)	ns
Clinical risk factors			
Hypertension	62 (59%)	43 (41%)	0.009
Hypercholesterolemia	43 (41%)	47 (44%)	ns
Current smoker	32 (30%)	51 (48%)	0.007
Diabetes mellitus	8 (8%)	9 (9%)	ns
Family history of coronary artery disease	56 (53%)	52 (49%)	ns
Obesity	12 (11%)	17 (16%)	ns
Presenting symptom			
Atypical chest pain	19 (18%)	106 (100%)	<0.001
Typical chest pain	58 (55%)
Breathlessness	27 (25%)
Syncope	2 (2%)
ECG type of MI and troponin I peak			
NSTEMI or borderline ECG abnormalities	62 (58%)
STEMI	44 (42%)
Troponin I peak, median (lower-upper quartile) ng/mL	2.58 (1.23–7.17)
Echocardiography and CMR			
Reduced LVEF (<50%)	51 (48%)
Wall motion abnormality (CMR or echocardiography)	75 (71%)
CMR-LGE in at least 1 segment	56 (53%)
Infarct-related artery identified <i>excluding TTS*</i> , n (%)	49/80 (61%)
Infarct-related artery <i>excluding TTS*</i> , (RCA/LAD/Cx),* n	9/30/10
CCTA			
Agatston score, median (lower-upper quartile)	0 (0–39)	0 (0–0)	<0.001
High-risk coronary plaque, n (%)	55 (52)	33 (31)	<0.003
Average pFAI, mean (standard deviation)	−68.37 (8.29)	−78.03 (6.20)	<0.0001

High-risk coronary plaque was defined as at least 1 plaque showing at least 1 among the following: positive remodeling, napkin ring sign, spotty calcifications or low-attenuation plaque. BMI indicates body mass index; CAD, coronary artery disease; CCTA, coronary computed tomography angiography; CMR-LGE, cardiac magnetic resonance late gadolinium enhancement; Cx, left circumflex coronary artery; LAD, left anterior descending coronary artery; LVEF, left ventricular ejection fraction; MI, myocardial infarction; MINOCA, myocardial infarction with nonobstructive coronary arteries; NSTEMI, non-ST-segment-elevation myocardial infarction; ns, not significant; pFAI, pericoronary fat attenuation index; RCA, right coronary artery; STEMI, ST-segment-elevation myocardial infarction; TTS, Tako-Tsubo syndrome.

*Infarct-related artery was assessed only for the 80 MINOCA, since not applicable in the 26 TTS, by definition not demonstrating an IRA.

fat volume was associated, but inversely, with mean pFAI only in the left anterior and left circumflex coronary arteries ($r=-0.429$, $r=-0.451$, $P<0.0001$), while this was not the case ($r=0.008$, $P=0.938$) for the right coronary artery. A significant correlation was instead seen in the control group for all 3 coronary arteries. Table 2 shows that mean pFAI on a coronary artery, which is identified as IRA for a given MINOCA event, trended to higher values compared with the mean pFAI value in the same coronary artery, when it is not deemed as

the IRA, although differences were not statistically significant ($P=ns$). After dividing the MINOCA/TTS group into MINOCA with no mechanism identified, SCAD, and TTS, mean pFAI in each of the 3 subgroups was significantly higher than mean pFAI in controls ($P<0.0001$ or $P<0.001$), but mean pFAI values among the 3 MINOCA/TTS subgroups were not significantly different when compared among them (Figure 3).

From the receiver operating characteristic analysis ≥ -70.83 HU was derived as the best pFAI cutoff associated

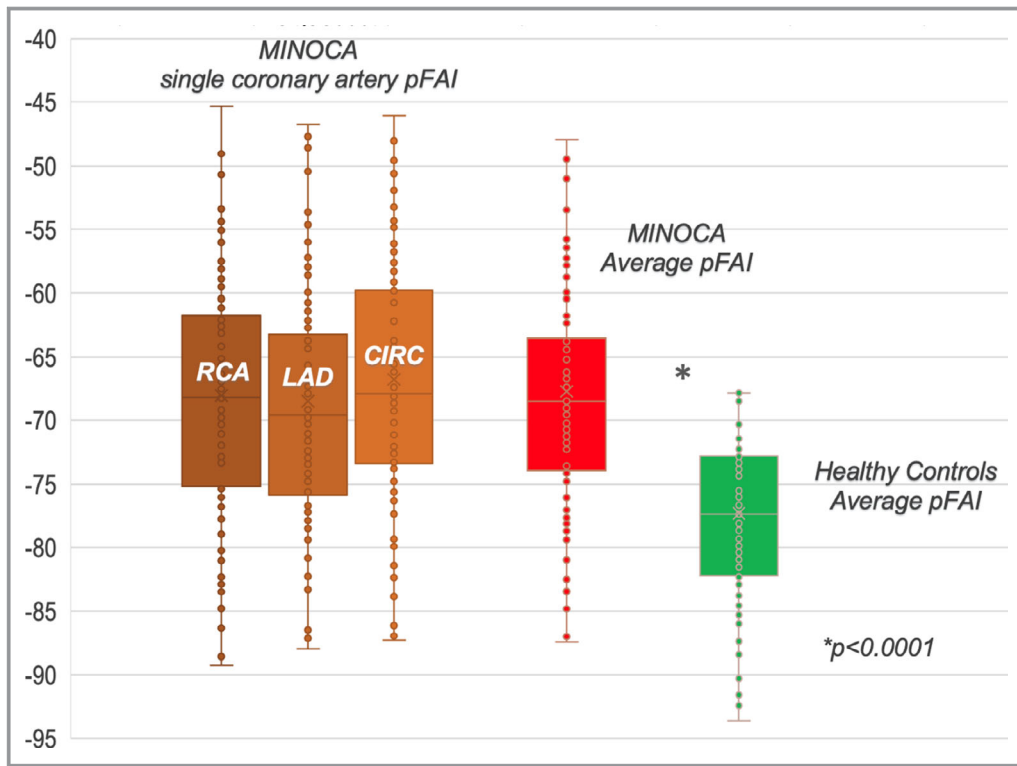


Figure 1. Individual coronary artery pFAI in MINOCA, and average values in myocardial infarction with nonobstructive coronary arteries (MINOCA) and controls. CIRC indicates left circumflex coronary artery; LAD, left anterior descending coronary artery; pFAI, pericoronary fat attenuation index (measured in Hounsfield units); RCA, right coronary artery.

with MINOCA/TTS (versus control group), with an area under the curve=0.823, sensitivity=0.613 (95% CI, 0.514–0.706), and specificity=0.924 (95% CI, 0.857–0.967).

When defining inflammation as pFAI ≥ -70.1 HU, as previously reported in subjects with stable CAD⁵ (and closely replicated in the current data set, with best cutoff value

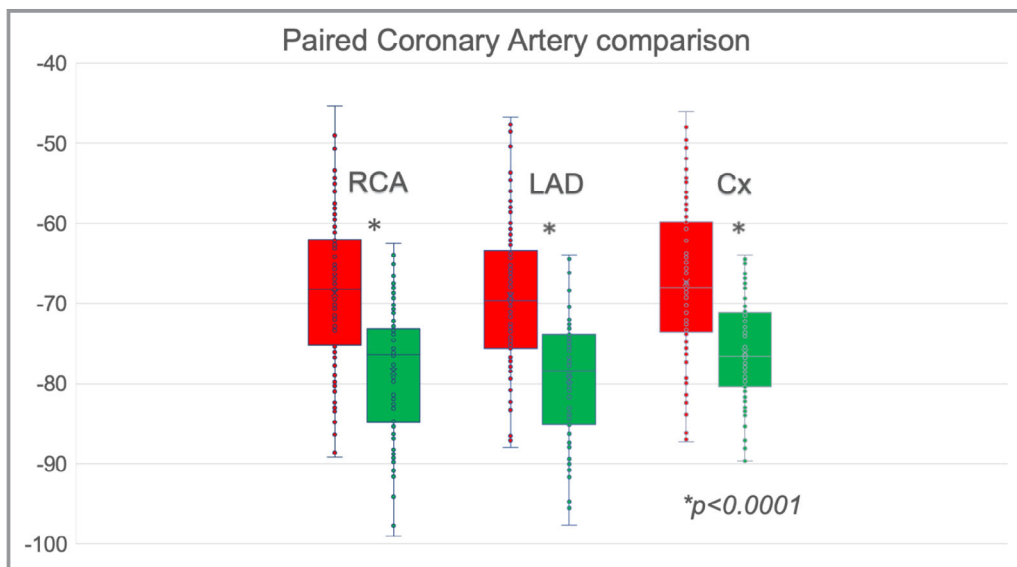


Figure 2. Myocardial infarction with nonobstructive coronary arteries (MINOCA) (red) and controls (green) pFAI paired comparison in single coronary arteries. Cx indicates left circumflex coronary artery; LAD, left anterior descending coronary artery; pFAI, pericoronary fat attenuation index (measured in Hounsfield units); RCA, right coronary artery.

Table 2. CCTA Data in MINOCA/TTS and Controls

CCTA Coronary Plaque Data		MINOCA/TTS (n=106)		Controls (n=106)		P for Difference	
Number of patients with at least 1 coronary plaque (any type)		64		42		0.004	
High-risk positive remodeling		50		27		0.002	
High-risk spotty calcifications		30		20		0.145	
High-risk napkin-ring sign		26		14		0.053	
High-risk low attenuation plaque		29		5		<0.0001	
At least 1 of the high-risk (above-mentioned) characteristics		55		33		0.003	
CCTA pFAI Data		RCA	LAD	Cx	RCA	LAD	Cx
Available data, n		106	103	102	105	105	104
Fat volume, mL, mean (SD)		1.27 (0.51)	1.24 (0.44)	0.73 (0.35)	1.23 (0.45)	1.22 (0.45)	0.78 (0.34)
Fat attenuation, HU, mean		−68.71	−69.06	−67.38	−78.51	−79.49	−76.15*
Fat attenuation, HU, SD		9.88	9.13	9.91	8.401	8.14	6.47
Infarct-Related Artery (TTS Excluded) n=49 of n=80 MINOCA							
pFAI in the coronary artery when labeled as IRA, HU, mean (SD)		−61.89 (11.88)		−67.75 (7.69)		−65.71 (10.47)	
P for difference		0.11		0.56		0.87	
pFAI in the coronary artery when not labeled as IRA, HU, mean (SD)		−68.75 (8.22)		−69.32 (10.04)		−66.30 (10.01)	

CCTA indicates coronary computed tomography angiography; Cx, left circumflex coronary artery; IRA, infarct-related artery; LAD, left anterior descending coronary artery; MINOCA, myocardial infarction with nonobstructive coronary arteries; pFAI, pericoronary fat attenuation index (in Hounsfield units [HU]); RCA, right coronary artery; TTS, Tako-Tsubo syndrome. * $P<0.05$ compared with RCA and LAD of the control group.

−70.83 HU), 55% of MINOCA/TTS were demonstrated to have inflamed coronary arteries, while coronary inflammation was found in only 5% of controls, as shown in Figure 4. High-risk plaques were found in 32 of the 59 (54%) patients with pFAI >−70.1 HU and 23 of the 48 (48%) with pFAI <−70.1 ($P=ns$).

Intra- and Interobserver Agreement

Intraclass correlation coefficient between 2 separate sets of pFAI measurements (average of the 3 coronary arteries) performed by the same operator (BB) on 60 random exams (30 MINOCA and 30 controls), was 0.892, while the same parameter assessed between 2 different readers (BB and CM), for the same 60 exams, was 0.844; both values of intra- and interrater agreement are generally classified as good to excellent.

Discussion

To our knowledge, this is the first study reporting on coronary inflammation in patients with MINOCA/TTS using the CCTA pericoronary fat attenuation method, and comparing data versus a control group with no obstructive CAD and no cardiac events in their follow-up. Our main findings indicate that mean pFAI in MINOCA/TTS is significantly higher than in controls, either comparing the average pFAI measurement of the 3 coronary arteries or pFAI in each single coronary artery. Evidence is rapidly accumulating that higher pFAI mirrors coronary inflammation,^{3–5,7}

so that we may conclude that coronary arteries are affected by inflammation in MINOCA/TTS. Whether this inflammatory process is causative or just the downstream effect of another primary causative process in MINOCA/TTS is out of the scope of the current study. Figure 5 shows 2 paradigmatic examples of pFAI measurements on the right coronary artery in a patient with MINOCA and a control patient. We also found a statistically significant higher prevalence of (nonobstructive) coronary artery plaques in general, but more specifically of high-risk plaques in patients with MINOCA/TTS compared with the control group, the difference being particularly striking regarding low-attenuation plaques, almost 6 times more frequent in patients with MINOCA/TTS. Regarding the comparison of total plaque burden, the finding is in discordance with the only prior study, in a smaller sample, reporting on the comparison between patients with MINOCA and healthy controls,¹⁴ while regarding the presence of high-risk plaques this is apparently the first report addressing the issue. We conclude that patients with MINOCA/TTS more frequently have coronary artery plaques, although nonobstructive, which are more frequently so-called high-risk plaques compared with subjects with no CAD or nonobstructive disease, and additionally showing no cardiac events in their follow-up (controls).

MINOCA/TTS Subgroups

Depending on the definition used for MINOCA,^{6,8} this entity may or may not include TTS, so that we also separately classified 3 subgroups of patients with MINOCA/TTS, either

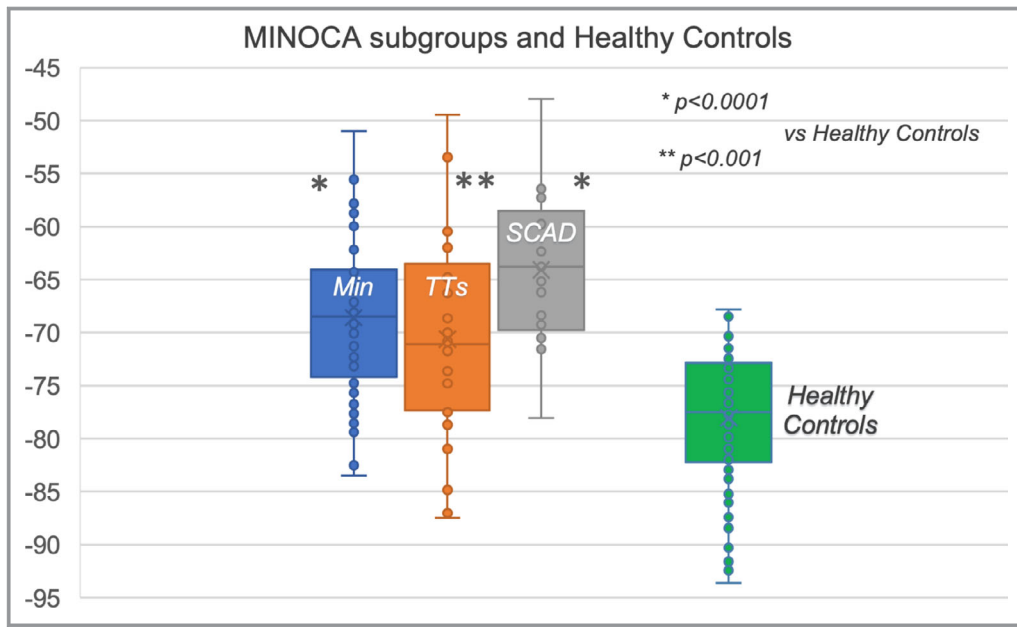


Figure 3. pFAI in myocardial infarction with nonobstructive coronary arteries (MINOCA) subgroups and average pFAI compared with controls. Min indicates MINOCA with no identifiable cause; pFAI, pericoronary fat attenuation index (measured in Hounsfield units); SCAD, suspected coronary artery dissection; TTs, Tako-Tsubo syndrome.

patients with MINOCA in whom no cause was suspected or patients with SCAD or with TTS, to determine whether mean pFAI differed among 3 such broad categories of patients with nontypical MI (and how they compare with healthy controls). With the limitation of smaller subgroups for TTS and SCAD, there seems to be a mild gradient of decreasing inflammation (pFAI) from SCAD through MINOCA with no identifiable cause, to TTS, but this difference was statistically significant; on the contrary, a significant difference (with higher pFAI) was found when comparing pFAI of each of the 3 MINOCA/TTS subgroups versus controls.

It has been suggested that pFAI is also regionally modified (higher pFAI) in proximity of a culprit coronary artery plaque.^{3,4} In

our MINOCA/TTS cases, as per definition, there could not be any clearly identifiable culprit plaque; consequently, rather than using the culprit plaque assessment, we compared pFAI in the IRA versus pFAI measured in the same coronary artery when the other coronary arteries were instead identified as the IRA (see Table 2). A trend toward higher mean pFAI was recorded when the measured coronary was identified as the IRA (in particular for the right coronary artery), although we did not find statistically significant differences for such comparison, in any of the 3 coronary arteries. We assessed IRA, defined as the coronary artery subtending the myocardium with LGE or wall motion abnormalities, only in the 80 patients with MINOCA (not in the 26 TTS patients, in whom wall motion abnormalities typically cross the boundaries of coronary territories), and only in 49 IRA was finally assigned, so that the samples to be compared (and power) were rather small. From our data we can only conclude that coronary inflammation in MINOCA appeared more as a generalized process in the coronary artery tree of the patient, rather than a regionally limited process to a specific target coronary artery.

This is, to our knowledge, the first study reporting on pFAI in MINOCA and TTS, and while it is a novel contribution to research, it is only the first piece of information regarding the assessment of relatively rare entities such as MINOCA/TTS using this new pFAI inflammatory marker, and it should be replicated in other studies.

pFAI is easy to use clinically and, importantly, it is easily retrospectively measurable from the same standard CCTA,

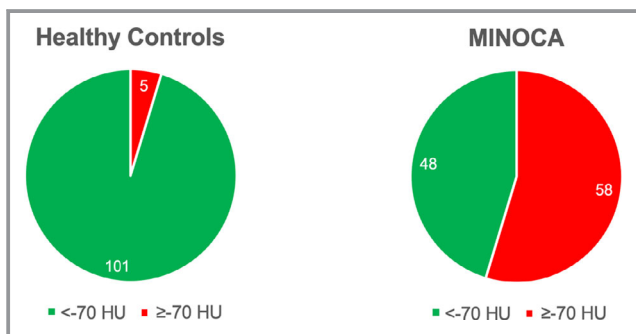


Figure 4. Distribution of coronary inflammation (red), defined as average pFAI ≥ -70 in controls (left) and myocardial infarction with nonobstructive coronary arteries (MINOCA) (right). pFAI indicates pericoronary fat attenuation index (measured in Hounsfield units [HU]).

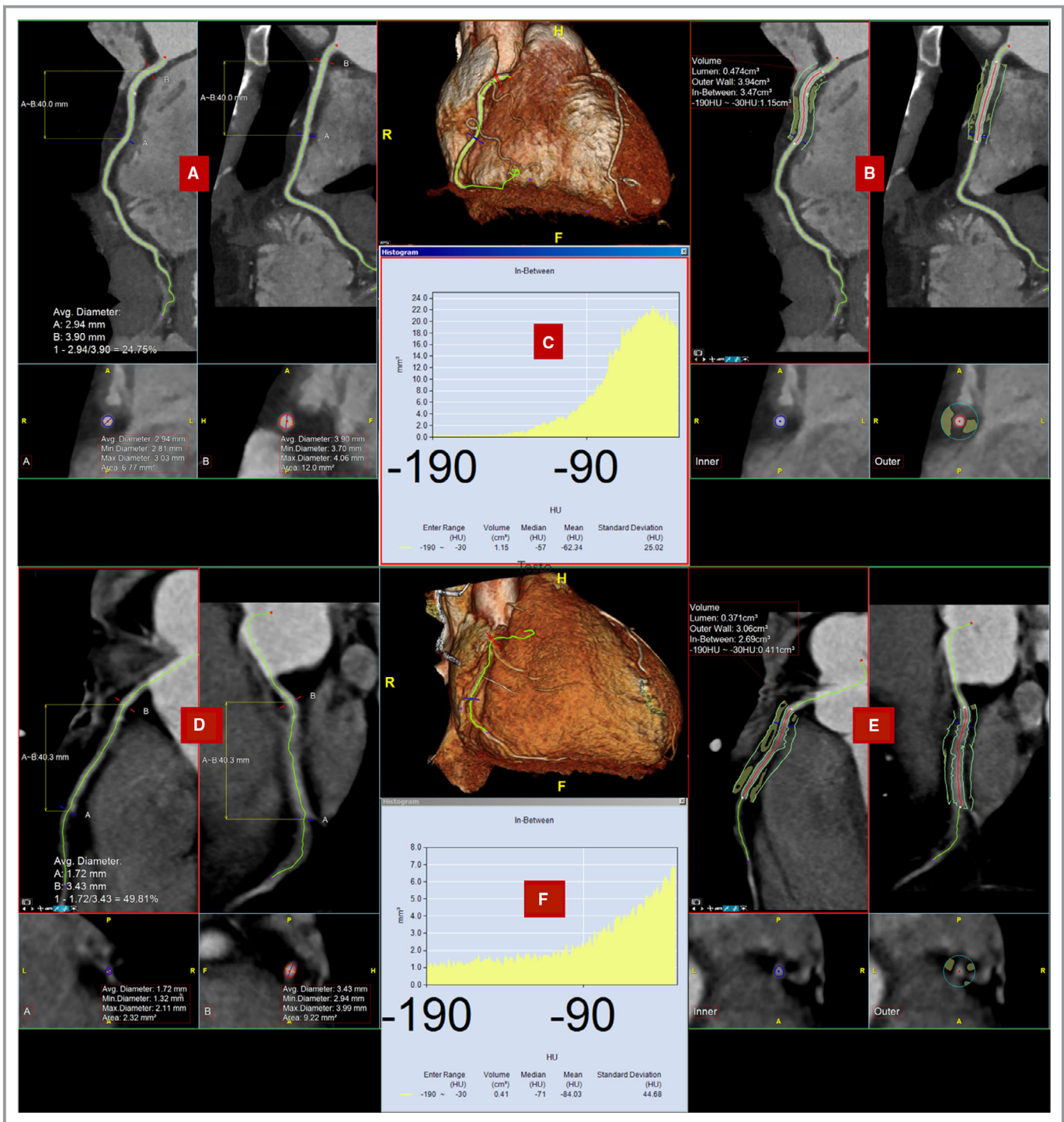


Figure 5. Two exams, the upper one in a patient with MINOCA and the lower one in a control subject. **A** and **B**, The initial identification of the tract of the right coronary artery to be measured, selecting the tract 10 to 50 mm from the coronary ostium distally (40 mm are measured); in **(B** and **E)** the outer boundary of the volumetric sample is increased of the same length as the coronary artery diameter, to include pericoronary fat, which is then measured in **(C** and **F)** (histograms) for its mean radiodensity (C=−62.34 HU in MINOCA, C1=−84.03 HU in the control). HU indicates Hounsfield units.

which may highlight other important information regarding the presence of high-risk plaques, for example, apparently more frequent in MINOCA/TTS. A recent paper on TTS has clearly

demonstrated macrophage-mediated cellular inflammatory response in the myocardium, superimposed on myocardial edema, and the authors showed systemic peripheral

inflammatory responses, some of which appear to persist for months.¹⁵ Such data confirm inflammatory responses in TTS, as we have also demonstrated more specifically in the coronary arteries using pFAI measurement, not only in TTS but also in the other patients with MINOCA. Vasospasm, widely recognized as one of the causes of MINOCA, has also been recently linked to coronary inflammation.⁷

Coronary inflammation is becoming clinically demonstrable in different types of coronary artery disease, and is consequently a candidate to become a key target for future therapeutic strategies.¹⁶

The medical literature is flooded with clinical and imaging variables that, once categorized, for example, in quartiles, are finally proven diagnostic or prognostic markers, but such variables are often difficult to use in the clinical field because of the unavailability of a robust “yes/no” cutoff value. We find it interesting that, as far as pFAI is concerned, -70 HU appears to be a reasonably robust cutoff to define the coronary arteries as inflamed or not (at least in the assessment of their proximal 40-mm tract); in fact, this is the second study finding a best cutoff value close to the -70 HU threshold.⁵ A third study performed in a small group of patients with acute coronary syndrome found values not far from this -70 HU threshold, in this case used to differentiate culprit versus nonculprit plaques (-68.2 HU), notwithstanding the different clinical setting, the analysis not being limited to the proximal coronary segments, and the different software used for postprocessing.¹⁷

Further studies will confirm whether such -70 HU value is clinically applicable as a coronary inflammatory marker across different clinical scenarios.

Study Limitations

The study is retrospective and from a single center, with all inherent limitations; the early interest and involvement of our center’s cardioradiology group in research on TTS¹⁸ and MINOCA¹⁹ has favored the use of CCTA and CMR in clinical routine for such patients with suspected MI without obstructive CAD, leading to 118 of 177 patients with MINOCA/TTS admitted during the study period (67%) having both CCTA and CMR available, with 106 patients with MINOCA/TTS finally enrolled. Drug therapy was not recorded in the current study because it was deemed difficult to interpret, as patients with MINOCA/TTS are typically treated from day 0 of hospital admission as suspected acute coronary syndromes, with high-dose statins, beta-blockers, angiotensin-converting enzyme inhibitors/angiotensin receptor blockers, dual antiplatelet therapy, and low-molecular-weight heparin or fondaparinux, but they also have prior chronic and unrecorded therapies. CCTA was performed a few days after admission, and the relative contribution of chronic versus recent therapies to the measurement of pFAI is impossible to weigh. For this reason, we

cannot exclude an effect of drugs used in acute coronary syndromes on pFAI in our MINOCA/TTS group, although high-dose statins, immediately prescribed in suspected acute coronary syndromes, for example, are expected to bear an opposite (anti-inflammatory) effect, more probably reducing inflammation (and possibly the difference in pFAI) between MINOCA/TTS and controls, rather than the opposite. Vasomotor tests, intracoronary ultrasonography, optical coherence tomography for in-depth coronary function, and plaque morphology assessments were not performed. However, these are invasive and time-consuming techniques that can hardly be used in clinical routine, limiting their clinical applicability to research, differently from pFAI measurement and CCTA plaque assessment.

Conclusions

In patients with MINOCA and TTS, CCTA is not only able to detect otherwise angiographically invisible high-risk plaques, which are apparently more frequently diagnosed than in controls, but CCTA diagnostic yield can be further extended by attenuation characterization of pericoronary fat tissue. MINOCA/TTS cases clearly demonstrated higher pFAI, a surrogate for coronary inflammation, in comparison with controls. We speculate that pFAI diagnostic data in the future may also help better select patients for new therapies, for example, targeting coronary inflammation.

Disclosures

None.

References

- Ross R. Atherosclerosis—an inflammatory disease. *N Engl J Med*. 1999;340:115–126.
- Harrington RA. Targeting inflammation in coronary artery disease. *N Engl J Med*. 2017;377:1197–1198.
- Antonopoulos AS, Sanna F, Sabharwal N, Thomas S, Oikonomou EK, Herdman L, Margaritis M, Shirodaria C, Kampoli AM, Akoumianakis I, Petrou M, Sayeed R, Krasopoulos G, Psarros C, Ciccone P, Brophy CM, Digby J, Kelion A, Uberoi R, Anthony S, Alexopoulos N, Tousoulis D, Achenbach S, Neubauer S, Channon KM, Antoniades C. Detecting human coronary inflammation by imaging perivascular fat. *Sci Transl Med*. 2017;9:eaa12658.
- Kwiecinski J, Dey D, Cadet S, Lee SE, Otaki Y, Huynh PT, Doris MK, Eisenberg E, Yun M, Jansen MA, Williams MC, Tamarappoo BK, Friedman JD, Dweck MR, Newby DE, Chang HJ, Slomka PJ, Berman DS. Peri-Coronary Adipose Tissue Density Is Associated with (18)F-sodium Fluoride Coronary Uptake in stable Patients with High-Risk plaques. *JACC Cardiovasc Imaging*. 2019. pii:S1936-878X(19)30076-2. DOI: 10.1016/j.jcmg.2018.11.032. [Epub ahead of print]. PubMed PMID: 30772226; PubMed Central PMCID: PMC6689460.
- Oikonomou EK, Marwan M, Desai MY, Mancio J, Alashi A, Hutt Centeno E, Thomas S, Herdman L, Kotanidis CP, Thomas KE, Griffin BP, Flamm SD, Antonopoulos AS, Shirodaria C, Sabharwal N, Deanfield J, Neubauer S, Hopewell JC, Channon KM, Achenbach S, Antoniades C. Non-invasive detection of coronary inflammation using computed tomography and prediction of residual cardiovascular risk (the CRISP CT study): a post-hoc analysis of prospective outcome data. *Lancet*. 2018;392:929–939.
- Agewall S, Beltrame JF, Reynolds HR, Niessner A, Rosano G, Caforio AL, De Caterina R, Zimarino M, Roffi M, Kjeldsen S, Atar D, Kaski JC, Sechtem U,

- Tornvall P; on behalf of the Working Group on Cardiovascular Pharmacotherapy. ESC working group position paper on myocardial infarction with non-obstructive coronary arteries. *Eur Heart J*. 2017;38:143–153.
7. Ohyama K, Matsumoto Y, Takanami K, Ota H, Nishimiya K, Sugisawa J, Tsuchiya S, Amamizu H, Uzuka H, Suda A, Shindo T, Kikuchi Y, Hao K, Tsuburaya R, Takahashi J, Miyata S, Sakata Y, Takase K, Shimokawa H. Coronary adventitial and perivascular adipose tissue inflammation in patients with vasospastic angina. *J Am Coll Cardiol*. 2018;71:414–425.
 8. Tamis-Holland JE, Jneid H, Reynolds HR, Agewall S, Brilakis ES, Brown TM, Lerman A, Cushman M, Kumbhani DJ, Arslanian-Engoren C, Bolger AF, Beltrame JF; American Heart Association Interventional Cardiovascular Care Committee of the Council on Clinical Cardiology; Council on Cardiovascular and Stroke Nursing; Council on Epidemiology and Prevention; and Council on Quality of Care and Outcomes Research. Contemporary diagnosis and management of patients with myocardial infarction in the absence of obstructive coronary artery disease: a scientific statement from the American Heart Association. *Circulation*. 2019;139:e891–e908.
 9. Ghadri JR, Wittstein IS, Prasad A, Sharkey S, Dote K, Akashi YJ, Cammann VL, Crea F, Galiuto L, Desmet W, Yoshida T, Manfredini R, Eitel I, Kosuge M, Nef HM, Deshmukh A, Lerman A, Bossone E, Citro R, Ueyama T, Corrado D, Kurisu S, Ruschitzka F, Winchester D, Lyon AR, Omerovic E, Bax JJ, Meimoun P, Tarantini G, Rihal C, Y-Hassan S, Migliore F, Horowitz JD, Shimokawa H, Lüscher TF, Templin C. International expert consensus document on Takotsubo syndrome (part I): clinical characteristics, diagnostic criteria, and pathophysiology. *Eur Heart J*. 2018;39:2032–2046.
 10. Cerqueira MD, Weissman NJ, Dilsizian V, Jacobs AK, Kaul S, Laskey WK, Pennell DJ, Rumberger JA, Ryan T, Verani MS; American Heart Association Writing Group on Myocardial Segmentation and Registration for Cardiac Imaging. Standardized myocardial segmentation and nomenclature for tomographic imaging of the heart: a statement for healthcare professionals from the Cardiac Imaging Committee of the Council on Clinical Cardiology of the American Heart Association. *Circulation*. 2002;105:539–542.
 11. Puchner SB, Liu T, Mayrhofer T, Truong QA, Lee H, Fleg JL, Nagurney JT, Udelson JE, Hoffmann U, Ferencik M. High-risk plaque detected on coronary CT angiography predicts acute coronary syndromes independent of significant stenosis in acute chest pain: results from the ROMICAT-II trial. *J Am Coll Cardiol*. 2014;64:684–692.
 12. Bondarenko O, Beek AM, Hofman MB, Kuhl H, Twisk J, Van Dockum WG, Visser CA, Van Rossum A. Standardizing the definition of hyperenhancement in the quantitative assessment of infarct size and myocardial viability using delayed contrast-enhanced CMR. *J Cardiovasc Magn Reson*. 2005;7:481–485.
 13. Friedrich MG, Sechtem U, Schulz-Menger J, Holmvang G, Alakija P, Cooper LT, White JA, Abdel-Aty H, Gutberlet M, Prasad S, Aletras A, Laissy JP, Paterson I, Filipchuk NG, Kumar A, Pauschinger M, Liu P; International Consensus Group on Cardiovascular Magnetic Resonance in Myocarditis. Cardiovascular magnetic resonance in myocarditis: a JACC White Paper. *J Am Coll Cardiol*. 2009;53:1475–1487.
 14. Brolin EB, Jernberg T, Brismar TB, Daniel M, Henareh L, Ripsweden J, Tornvall P, Cederlund K. Coronary plaque burden, as determined by cardiac computed tomography, in patients with myocardial infarction and angiographically normal coronary arteries compared to healthy volunteers: a prospective multicenter observational study. *PLoS One*. 2014;9:e99783.
 15. Scally C, Abbas H, Ahearn T, Srinivasan J, Mezincescu A, Rudd A, Spath N, Yucel-Finn A, Yucel R, Oldroyd K, Dospinescu C, Horgan G, Broadhurst P, Henning A, Newby DE, Semple S, Wilson HM, Dawson DK. Myocardial and systemic inflammation in acute stress-induced (Takotsubo) cardiomyopathy. *Circulation*. 2019;139:1581–1592.
 16. Ridker PM, Everett BM, Thuren T, MacFadyen JG, Chang WH, Ballantyne C, Fonseca F, Nicolau J, Koenig W, Anker SD, Kastelein JJP, Cornel JH, Pais P, Pella D, Genest J, Cifkova R, Lorenzatti A, Forster T, Kobalava Z, Vida-Simiti L, Flather M, Shimokawa H, Ogawa H, Dellborg M, Rossi PRF, Troquay RPT, Libby P, Glynn RJ; CANTOS Trial Group. Antiinflammatory therapy with canakinumab for atherosclerotic disease. *N Engl J Med*. 2017;377:1119–1131.
 17. Goeller M, Tamarappoo BK, Kwan AC, Cadet S, Commandeur F, Razipour A, Slomka PJ, Gransar H, Chen X, Otaki Y, Friedman JD, Cao JJ, Albrecht MH, Bittner DO, Marwan M, Achenbach S, Berman DS, Dey D. Relationship between changes in pericoronary adipose tissue attenuation and coronary plaque burden quantified from coronary computed tomography angiography. *Eur Heart J Cardiovasc Imaging*. 2019;20:636–643.
 18. Gaibazzi N, Ugo F, Vignali L, Zoni A, Reverberi C, Gherli T. Tako-Tsubo cardiomyopathy with coronary artery stenosis: a case-series challenging the original definition. *Int J Cardiol*. 2009;133:205–212.
 19. Aldrovandi A, Cademartiri F, Arduini D, Lina D, Ugo F, Maffei E, Menozzi A, Martini C, Palumbo A, Bontardelli F, Gherli T, Ruffini L, Ardissino D. Computed tomography coronary angiography in patients with acute myocardial infarction without significant coronary stenosis. *Circulation*. 2012;126:3000–3007.

SUPPLEMENTAL MATERIAL

Data S1.

CCTA acquisition protocol with Dual-Source CT scanner (Definition, Siemens Medical Solutions, Forchheim, Germany): all patients underwent a single-beat FLASH scan before contrast administration for preliminary quantification of calcium score with the Agatston method and a dedicated software (CaScore; Siemens, Germany).

Coronary CT Angiography was performed in all patients with prospective ECG gating technique in patients with heart rate > 65 bpm. Patients with heart rate < 65 bpm were scanned with prospective ECG-triggered high-pitch “flash spiral” technique (pitch 3.2 and 3.4, table feed: 46 cm/s). High iodinate non-ionic contrast agent (400 mg iodine/ml; Iomeron, Bracco, Milan, Italy) was injected in all patients via an antecubital vein at 4–5 mL/s speed with automatic injector system (CT Stellant, Medrad Inc., Indianola, Pennsylvania) using well-known bolus tracking technique.

Automatic mAs values were obtained with the CareDose 4D option. CT acquisition parameters were as follows: slice collimation 3 mm × 128 × 0.6 mm with a z-flying focal spot; gantry rotation time 280 ms; pitch of 3.4; tube voltage of 100–120 kV (weight-based nomogram), and a tube current of 250–350 mAsref/rotation (topogram-based automatic reference tube current selection –CareDose 4D, Siemens Medical Solutions, Forchheim, Germany). All coronary CTA data sets were reconstructed with 0.75 mm slice thickness, 0.4 mm increment.

Images were reconstructed using sinogram affirmed iterative reconstruction (SAFIRE) with a specific cardiac tissue convolution kernel (I36f).

Image analysis. The following parameters were considered: plaque localization, plaque type, maximum plaque area, vessel stenosis, minimal noncalcified plaque attenuation, and the presence/absence of spotty calcifications. Noncalcified coronary atherosclerotic plaque was defined as any discernible structure that could be assigned to the coronary artery wall, had a CT density that was less than that of the contrast-enhanced coronary lumen and greater than that of the surrounding

epicardial fatty tissue, and could be identified in at least 2 independent planes.²⁰ Calcified atherosclerotic plaque was defined as any structure with a density of ≥ 130 HU that could be assigned to the coronary artery wall, visualized separately from the contrast-enhanced coronary lumen (because it was embedded in noncalcified plaque or its density was greater than that of the contrast-enhanced lumen), and could be identified in at least 2 independent planes.

The display settings used for the lumen and plaque analyses were manipulated to achieve optimal separation between the vessel lumen, wall, and surrounding tissue and minimize blooming artifacts in the case of calcified plaques. A cross-sectional image of each coronary segment was created on multiplanar reconstructions perpendicularly to the center-line of the vessel. In the presence of coronary plaque, the outer vessel contour at the point of maximum plaque area was manually traced to measure the vessel area, which was also measured in a coronary segment without any detectable atherosclerosis proximal to the lesion and used as the reference vessel area.

pFAI. Proximal, 40 mm-long segments of all major three epicardial coronary vessels (right coronary artery[RCA], left anterior descending artery [LAD] and left circumflex artery [LCx]) were tracked using a dedicated CCTA analysis software (Aquarius Workstation® V.4.4.13, TeraRecon Inc., Foster City, CA, USA). To avoid the effects of the aortic wall, the most proximal 10 mm of the RCA were excluded and analysis was performed in the proximal 10-50 mm of the vessel, as previously described.¹¹ In the LAD and LCx, analysis was performed in the proximal 40 mm of each vessel. If the obtuse marginal was clearly a more dominant vessel than the LCx, analysis was performed extending into the former vessel. The left main coronary artery was not analysed because of its variable length and anatomy and because it may be absent. Following identification of the segment of interest, the lumen as well as the inner and outer wall border were tracked in an automated manner with additional manual optimization. pFAI was defined as the adipose tissue located within a radial distance from the outer vessel wall equal to the diameter of the respective vessel.¹¹ Voxel attenuation histograms were plotted and the weighted average attenuation of all voxels between -30 to -190 HU

(thresholds used for the definition of AT) within the PVAT volume was used for the calculation of FAI PVAT, following adjustment for tube voltage. Mean and standard deviation were then recorded as automatically provided by the software.

CMR protocol:

CMR imaging was performed with a 1.5-Tesla scanners (Achieva, version 2.6, Philips Medical Systems, Eindhoven, The Netherlands) using 8-channel phased array coil.

Balanced steady state free precession cine-MR (SSFP cineMR) images acquired during breath-hold in the standard fashion (short axis, two chamber and four chamber views); in order to quantify left ventricular volumes, a stack of multiple-planes oriented on short-axis view was acquired completely encompassing the heart from the cardiac base to the apex (Cine SSFP sequence parameters: TR 51.3, TE 1.21, a flip angle 45° , an 8 mm slice thickness, interslice gap of 2 mm, a matrix of 256×256 , a FOV ranging from 340 mm to 450 mm and a voxel size of $2.0 \times 1.3 \times 8.0$ mm).

Black-blood Short Tau Inversion Recovery T2-weighted (STIR T2w) imaging was adopted to detect myocardial edema using a triple inversion recovery preparation module (TR 2 R-to-R intervals, TE 75 ms, flip angle 180° , TI 170 ms, slice thickness 8 mm, no interslice gap, FOV 340–400 mm, matrix 256×256).

Early enhancement was assessed using a free-breathing ECG-gated turbo spin echo T1-weighted (TSE T1w) sequence, which was acquired in four slices on short-axis view (basal, mid-basal, mid-apical and apical) both before and within the first 3 min after intravenous injection of contrast agent. The acquisition time for the sequence varied depending on the heart rate.

Contrast enhancement was achieved with the infusion of a single bolus of 0.2 mmol/kg of gadobenate dimeglumine (Multihance®, Bracco, Milan Italy) at 2 mL/s, followed by 15 mL of saline flush. TSE T1w sequences were acquired using only the body coil to compare the relative signal intensities of myocardium and skeletal muscle because body coils are known to give a more homogeneous signal. Specific TSE T1w sequence parameters were as follows: TR 500 ms; TE 23

ms; matrix, 320×192 ; FOV ranging from 340 to 450 mm; flip angle: 160 ms; slice thickness, 8.0 mm; slice spacing, 2.0 mm; acquisition time: 2–4 min depending on patient's heart rate.

Contrast-enhanced inversion recovery T1-weighted (IR-CE T1w) sequence was acquired in the late phase, 15 min after contrast injection, during breath-hold at end-diastole (IR-CE T1w sequence parameters: TR 9.6/4.4; matrix, 256×208 ; FOV 340–450 mm; flip angle, 25° ; slice thickness, 8.0 mm; and slice spacing, 2.0 mm); inversion time to null normal myocardium signal was 250–300 ms.

CMR Image Analysis As described in the White Paper document (1), myocardial edema was assessed as regions with signal intensity more than 2 standard deviations above the mean value of normal myocardium or a global increase of T2 signal with a ratio of more than 1.9, using skeletal muscle as reference. Late gadolinium enhancement (LGE) was defined as an increase of signal intensity >5 standard deviations above the remote myocardium, presenting a non-ischemic pattern of distribution (i.e. sub-epicardial or mesocardial enhancement). In this consensus document, the authors recommend a diagnosis of myocarditis when two out of three diagnostic criteria (known as “Lake Louise Criteria”) for tissue inflammation are satisfied. The three criteria in question are: 1. presence of late enhanced myocardial zones with non-coronary distribution, 2. presence of regional or diffuse myocardial edema and 3. presence of myocardial hyperemia and capillary leakage assessed by early gadolinium enhancement.

Supplemental Reference:

1. Friedrich MG, Sechtem U, Schulz-Menger J, Holmvang G, Alakija P, Cooper LT, White JA, Abdel-Aty H, Gutberlet M, Prasad S, Aletras A, Laissy JP, Paterson I, Filipchuk NG, Kumar A, Pauschinger M, Liu P; International Consensus Group on Cardiovascular Magnetic Resonance in Myocarditis. Cardiovascular magnetic resonance in myocarditis: A JACC White Paper. *J Am Coll Cardiol.* 2009;53:1475-87.